AD 460878

(1)

UNSTABLE OPTICAL RESONATORS FOR LASER APPLICATIONS

by

A. E. Siegman

Internal Memorandum
M. L. Report No. 1227
Contract AF 33(615)-1411
with partial support by
Contract DA 36(039) SC-90839
September 1964,

Microwave Laboratory
W. W. Hansen Laboratories of Physics
Stanford University
Stanford, California

12996

UNSTABLE OPTICAL RESONATORS FOR LASER APPLICATIONS

A. E. Siegman

Electrical Engineering Department
and Microwave Laboratory,
Stanford University, California 94305

ABSTRACT

A simple geometrical analysis has been developed which describes the lowest-order transverse mode in an arbitrary unstable optical resonator of large Fresnel number. The lowest mode is assumed to consist of two oppositely traveling spherical waves which uniformly illuminate the two end mirrors. The centers of curvature of these two waves (which are not in general the mirror centers of curvature) are found by requiring that each center be the image of the other upon reflection from the appropriate spherical end mirror. The resonator losses, found from simple geometrical considerations, are given by simple analytical expressions and are entirely independent of the mirror sizes. The equi-loss contours on the usual mode chart are hyperbolae. The present results agree well with more exact results calculated by Fox and Li for the unstable case, and with experimental results on a ruby laser having a divergent spherical surface ground directly onto the ruby rod. Unstable resonators of this type appear potentially useful for transverse mode control and for diffraction output coupling.

TABLE OF CONTENTS

LIST OF FIGURES

INTRODUCTION

Two flat or curved mirror surfaces erected facing each other form an optical resonator or resonant cavity. Resonators of this type have been extensively studied recently[1-15] because of their importance in laser applications. The properties of such resonators are found to depend strongly in particular upon the mirror curvatures relative to the mirror spacing. If the spacing between the two mirrors is L and the mirror radii of curvature are R_1 and R_2, as shown in the sketch of Fig. 1, it has been found to be convenient to define the normalized curvature or g parameters[3,6]

$$g_1 = 1 - L/R_1 \quad ; \quad g_2 = 1 - L/R_2 \quad .$$

The mode properties of optical resonators can then be summarized on the mode chart shown in Fig. 1, where any given resonator is represented by a single point somewhere on the chart.[3,6]

The mode chart is divided into stable (shaded) and unstable regions. The analytic condition

$$0 \leq g_1 g_2 \leq 1$$

defines the shaded stable region. It is well established that if a resonator lies well within the shaded stable region, its resonant modes

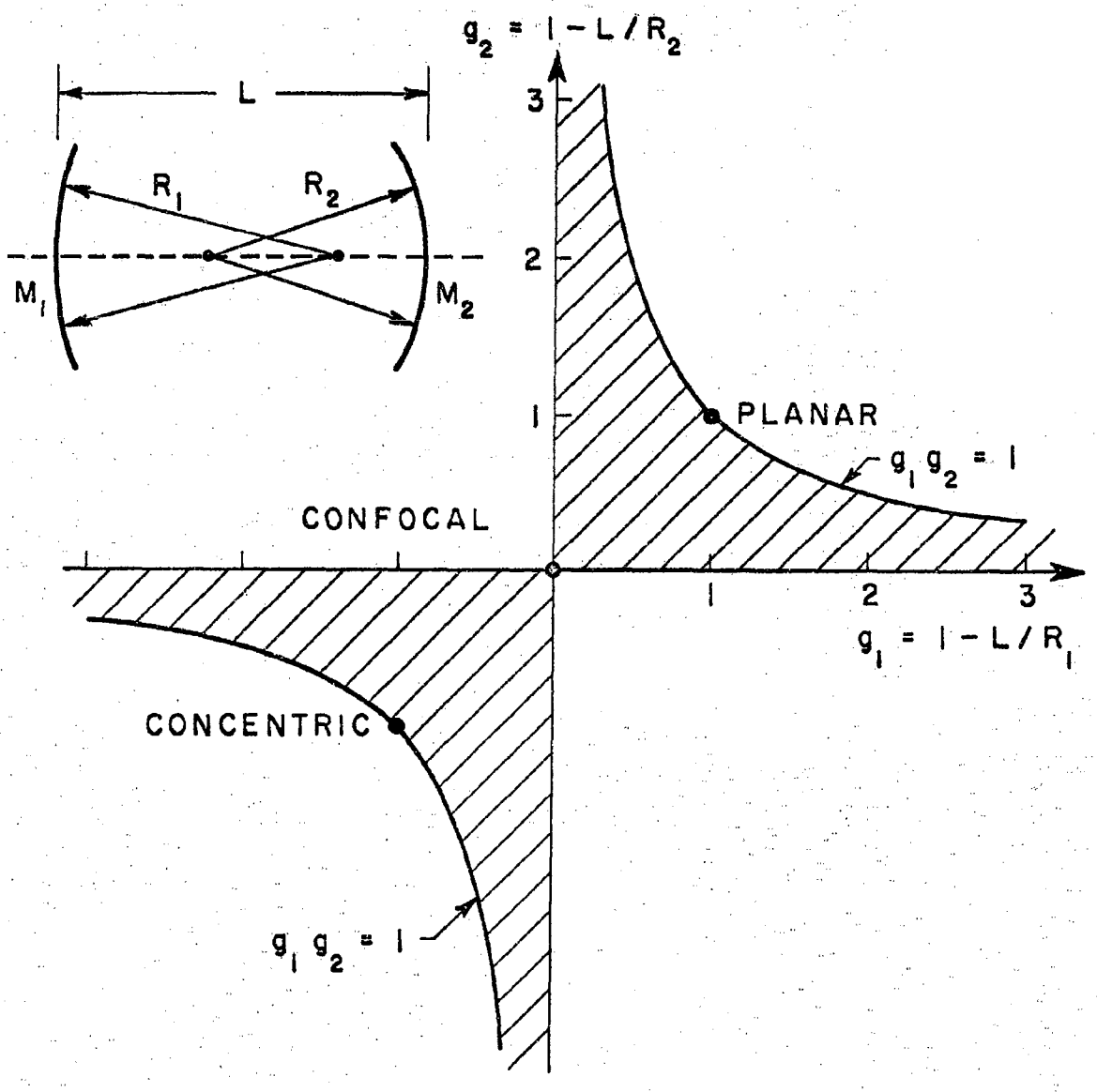

FIG. 1--A general optical resonator and the relevant mode chart which summarizes the mode stability properties. Resonators with g values well inside the shaded region are stable or low-loss; those well outside are unstable and have high losses.

can be found from a relatively exact closed-form analysis. The lowest-order resonant modes are, in general, narrowly confined along the axis of the resonator, the modes having gaussian transverse amplitude variations. The diffraction losses of such modes, i.e., the energy losses due to energy leakage out the sides or past the mirror edges, are generally very small.

Both the transverse dimensions of the modes and their diffraction losses increase for resonators located near or on the stable-region boundaries of the mode chart. The integral equations governing the resonant modes must then be solved either by iterative numerical computations[1-4] or by various analytic expansions.[11,15] In general, and speaking very roughly, the resonant modes are somewhat like the resonant waveguide modes which would appear if the resonator had conducting instead of open sides; and the diffraction losses increase rapidly as one passes through the stable-unstable boundary.

The chief contribution of this paper is a simple analysis, based on purely geometrical optical considerations, which predicts the lowest-order mode and its diffraction loss for large-Fresnel-number resonators located in the unstable region of the mode chart. The results of this analysis connect smoothly with the limited number of results which have been obtained previously, using iterative numerical procedures, for modes on the stable-unstable boundary.[4] In general, the diffraction losses in the unstable region turn out to be sizable, although not necessarily intolerable.

There is some practical interest in unstable resonators for laser applications. As a general principle, in order to obtain transverse mode selection, i.e., in order to obtain oscillation in a single lowest-order

transverse mode pattern, one must have sizable diffraction losses. Other loss mechanisms such as scattering and reflection are essentially the same for all modes, only the diffraction losses being different for different transverse modes. Hence, mode selection is obtained only if diffraction losses form a significant fraction of the total losses. This can be achieved in practice by using a stable resonator with small enough mirrors, or by using a resonator located in (but not too far into) the unstable region.

It has also been pointed out recently that efficient output coupling from a laser can be obtained by means of diffraction coupling, i.e., by employing the diffracted energy output from a laser resonator as the useful output.[16] High gain lasers require relatively heavy output coupling, i.e., relatively large diffraction losses, such as are obtained in the unstable region. We will present at the end of this paper some experimental results for a ruby laser employing an unstable resonator which verify the present theory and also illustrate useful ways in which diffraction coupling can be employed with a ruby or other high-gain laser.

ANALYSIS

We will carry out the analysis using the geometry of Fig. 2. The general approach can be outlined as follows. We hypothesize that the right-going wave leaving mirror M_1 is a spherical wave of uniform intensity whose virtual center lies at point P_1 (which is not in general the center of curvature of this mirror). This wave strikes and uniformly illuminates the second mirror M_2, from which a fraction of the original energy is reflected as a left-going uniform spherical wave coming from the virtual center P_2. This wave in turn must illuminate mirror M_1 and be reflected as if it had come from the original center P_1, thus closing the loop. The positions of the hypothetical virtual centers P_1 and P_2 are found by requiring self-consistency, i.e., by requiring that each virtual center be the image of the other upon reflection in the appropriate spherical mirror. We will discuss the justification for the assumption of uniform illumination in a later paragraph.

The positions of P_1 and P_2 relative to the mirrors are measured in terms of the mirror spacing L by the dimensionless factors r_1 and r_2 as shown in Fig. 2. These quantities are taken positive for outward displacements as shown, and negative for inward displacements. According to the sign convention used in resonator analyses, the mirror radii of curvature R_1 and R_2 are negative numbers for outward curvatures, such as those shown in Fig. 2. The requirements that P_1 and P_2 be each

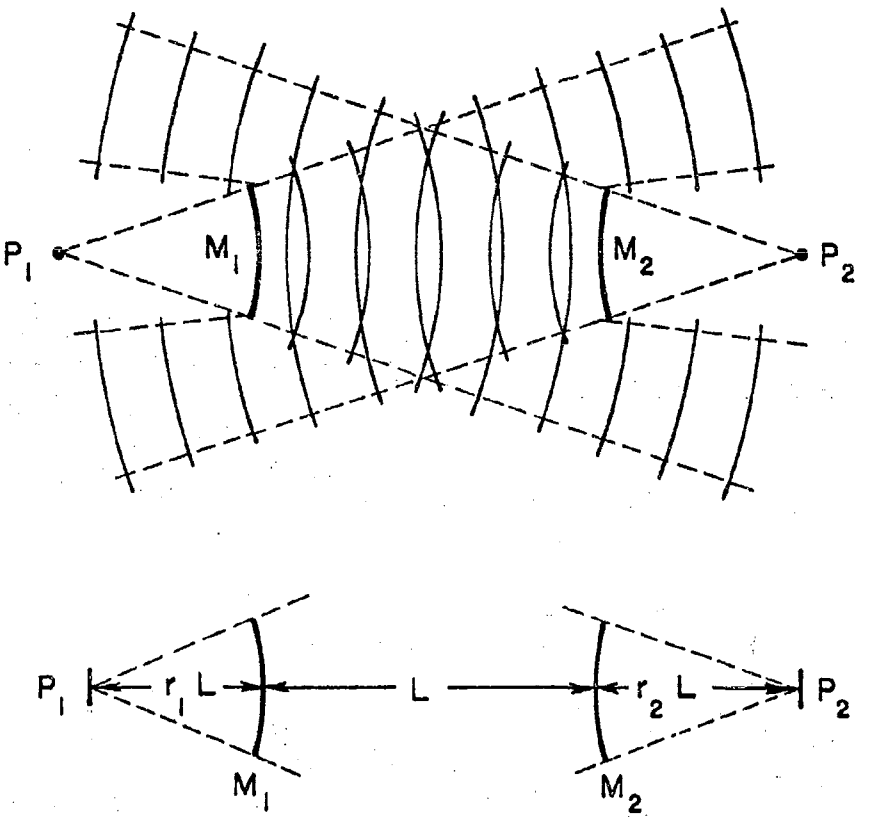

FIG. 2--Geometry used in analysing the unstable optical resonator case. The points P_1 and P_2 are the centers of curvature of the spherical wavefronts; these in general do not coincide with the centers of curvature of the mirrors.

other's images in the respective spherical surfaces are then expressed by the basic lens laws

$$\frac{1}{r_1} - \frac{1}{r_2 + 1} = -\frac{2L}{R_1} = 2(g_1 - 1)$$

$$\frac{1}{r_2} - \frac{1}{r_1 + 1} = -\frac{2L}{R_2} = 2(g_2 - 1) \quad .$$

Simultaneous solution of these two equations immediately yields the results

$$r_1 = \frac{\pm\sqrt{1 - (g_1 g_2)^{-1}} - 1 + g_1^{-1}}{2 - g_1^{-1} - g_2^{-1}}$$

$$r_2 = \frac{\pm\sqrt{1 - (g_1 g_2)^{-1}} - 1 + g_2^{-1}}{2 - g_1^{-1} - g_2^{-1}} \quad .$$

Further examination shows that only the upper sign before the radical represents a stable solution, in the sense that if one considers a small axial displacement of the position of one of the virtual centers away from the steady-state values above, then this small displacement will decrease with successive bounces for the upper sign, but will increase with successive bounces for the lower sign. Therefore, we consider only the upper sign.

The results just obtained are valid for the unstable regions in all quadrants of the mode chart, with r_1 and/or r_2 becoming negative outside the first quadrant. Figure 3 illustrates some of the resulting mode patterns for unstable resonators in various quadrants of the mode chart.

If we consider as a typical example the symmetric case $g_1 = g_2 = g$, the distance from the center of the resonator to either of the virtual centers can be written in physical terms as

$$r_1 L + L/2 = -\sqrt{|R|L/2 + (L/2)^2}$$

$$\approx -\sqrt{|R|L/2} \quad , \quad |R| \gg L \quad ,$$

where we assume that the radius of curvature $|R|$ will normally be much larger than the length L of the laser cavity. It appears that the distance to the virtual center is roughly the geometric mean of the radius of curvature and half the resonator length.

We have implicitly assumed in the above analysis that the mirror dimensions are large compared to an optical wavelength. In addition, we assume that the Fresnel number N commonly defined in resonator analyses is also large. If a mirror's transverse dimension is $2a$ (i.e., a strip of width $2a$ or a disc of diameter $2a$), the Fresnel number is defined as $N \equiv a^2/L\lambda$. We assume $N \gg 1$. In physical terms, this means that the number of Fresnel zones subtended by one mirror as seen from the other mirror surface is large.

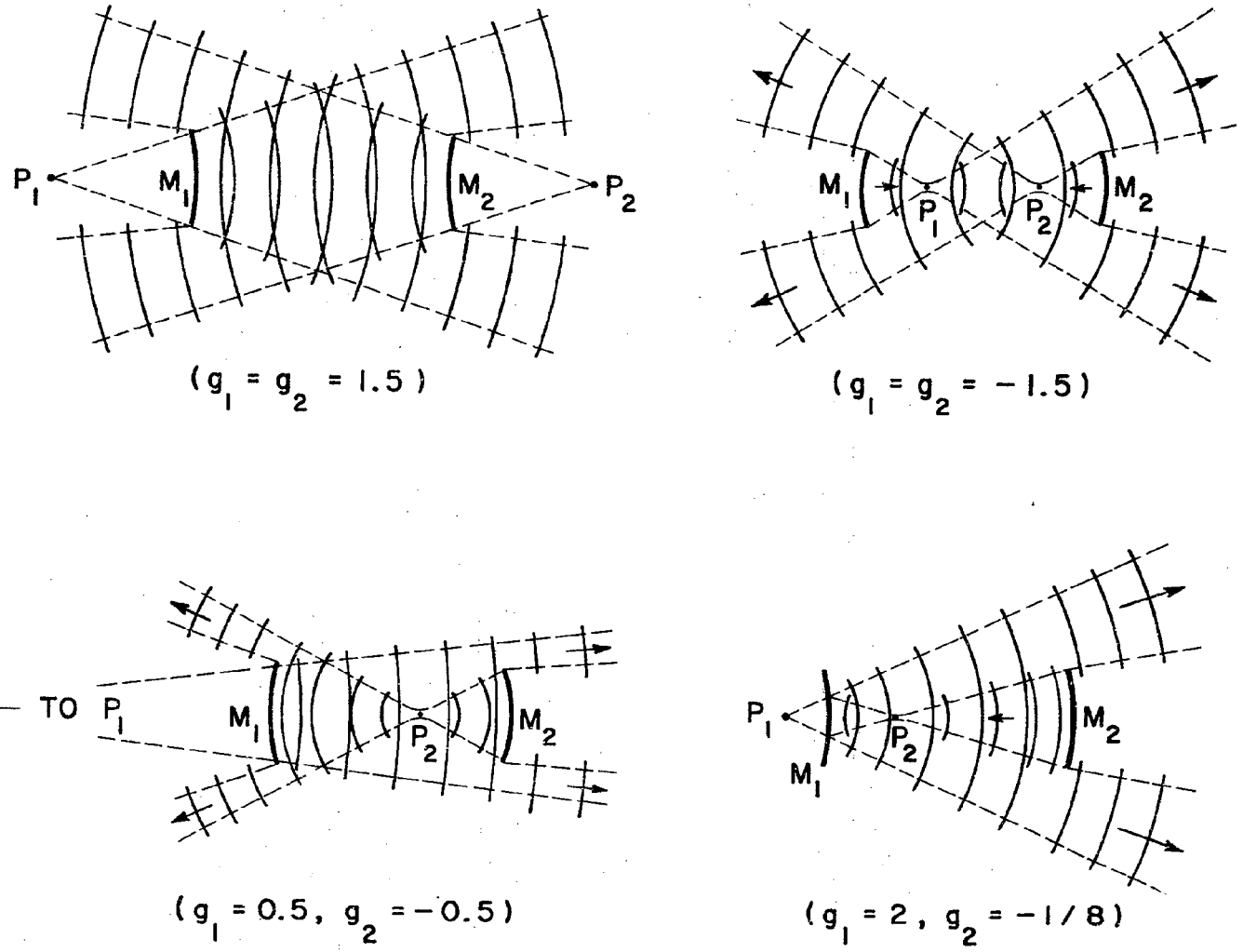

FIG. 3--Some typical mode patterns illustrating the unstable mode behavior in different unstable regions of the mode chart.

Within this assumption, it appears reasonable to assume uniform illumination of both mirrors, as illustrated in the sketches already given. It is clear that uniform illumination of either mirror will lead in turn to uniform illumination of the other mirror, except for diffraction effects due to the finite size of the first mirror. The large Fresnel number assumption means that such diffraction effects will be small.

DIFFRACTION LOSSES

The energy loss per bounce in these unstable resonators we obtain from a simple geometrical calculation of how much of the energy leaving one mirror misses striking the other mirror. We refer to these losses as diffraction losses even though it is clear that they are basically geometrical in origin. Diffraction in its usual sense plays no role, its chief effect being to cause some slight diffraction modification of the outer edges of the conical wave patterns, an effect which is ignored by the present analysis. The main justification for our terminology is that the losses calculated here connect smoothly with the losses in stable or nearly stable resonators, which are clearly the result of diffraction effects.

Assuming that a wave of unit intensity leaves mirror M_1, we will use Γ_1 to denote the fraction of its total energy reflected by mirror M_2, and $(1 - \Gamma_1)$ to denote the fraction which is lost. Similarly, Γ_2 is the fraction reflected from M_1 when unit intensity leaves M_2. The fractional intensity returning to either mirror after a complete round trip is thus $\Gamma^2 \equiv \Gamma_1\Gamma_2$.

There are several possible ways to define the "average power loss per bounce," which we will denote by $\bar{\delta}$, in an asymmetric resonator where the losses at the two ends may not be the same. For example, one reasonable definition might be the average of the two fractional losses, i.e.,

$$\bar{\delta} = \frac{1}{2}[(1 - r_1) + (1 - r_2)] \quad .$$

Alternatively, since the fractional power transmission in one round trip is $r^2 \equiv r_1 r_2$, the fractional power loss is 1 minus this, and dividing this equally among the two bounces in a round trip gives

$$\bar{\delta} = \frac{1}{2}(1 - r_1 r_2) = \frac{1}{2}(1 - r^2) \quad .$$

Finally, we note that if the one-way power gain along a laser is denoted by G , then the threshold condition for laser oscillation is $G^2 r_1 r_2 = G^2 r^2 = 1$. If this is written as $G(r_1 r_2)^{1/2} = Gr = 1$, it is clear that the average fractional transmission per pass is r and hence the average power loss per pass should be defined as

$$\bar{\delta} = (1 - r) = [1 - (r_1 r_2)^{1/2}] \quad .$$

For small fractional losses per bounce, these three definitions are essentially equivalent, but they differ significantly for large losses per bounce. Since the third of the above definitions seems to be the

most meaningful for laser discussions, it is the one we will employ in plotting our results. This is also the definition employed by Fox and Li.[1-4,20]

We consider first the strip mirror case in which the two mirrors are long parallel strips of infinite length and given width, with curvatures as indicated in the width direction only. It can then be shown from simple geometrical considerations that the round-trip fractional energy transmission is given by

$$r^2_{strip} = r_1 r_2 = \pm \frac{r_1 r_2}{(r_1 + 1)(r_2 + 1)} .$$

This expression does not contain any mirror sizes, and in fact detailed examination shows that the diffraction losses in the unstable region are entirely independent of mirror sizes, even in cases where one mirror is sufficiently large so that it is not fully illuminated and all of the losses are at the opposite end as in one of the sketches in Fig. 3. The upper sign in the r^2 expression is valid for g values in the unstable portions of the first and third quadrants of the mode chart, and the lower sign is valid in the other two quadrants.

Substitution of the expressions for r_1 and r_2 leads to the general result

$$r^2_{strip} = \pm \frac{1 - \sqrt{1 - (g_1 g_2)^{-1}}}{1 + \sqrt{1 - (g_1 g_2)^{-1}}} ,$$

with the same comments concerning signs. For the case of circular mirrors or discs, equally simple geometrical considerations lead to the result

$$\Gamma_{disc} = \Gamma^2_{strip} \quad ,$$

again independent of the sizes of the discs. It seems very likely in fact that these results hold for any arbitrary mirror shape. It would be a trivial exercise to extend these results to mirrors having different radii of curvature in two transverse directions. One can hypothesize that the resulting transmission would be

$$\Gamma^2_{general} = \pm \frac{r_1' \, r_1'' \, r_2' \, r_2''}{(r_1' + 1)(r_1'' + 1)(r_2' + 1)(r_2'' + 1)} \quad ,$$

where the primed and double-primed r values would correpond to the radii of curvature and the associated g values in the two transverse directions, using the same formulae as above to calculate the r values in terms of the g values.

Figures 4 and 5 summarize the average diffraction losses per bounce vs g for the two cases of a symmetric resonator with $g_1 = g_2 = g$. In order to compare these results with earlier results we have reproduced in Fig. 6 some results for diffraction losses vs Fresnel number N for several stable and unstable values of g obtained by Fox and Li using their iterative computer procedure.[4] The dashed lines which have been added to the figure are the results predicted by the present analysis. There appears to be good agreement between our results and the asymptotic

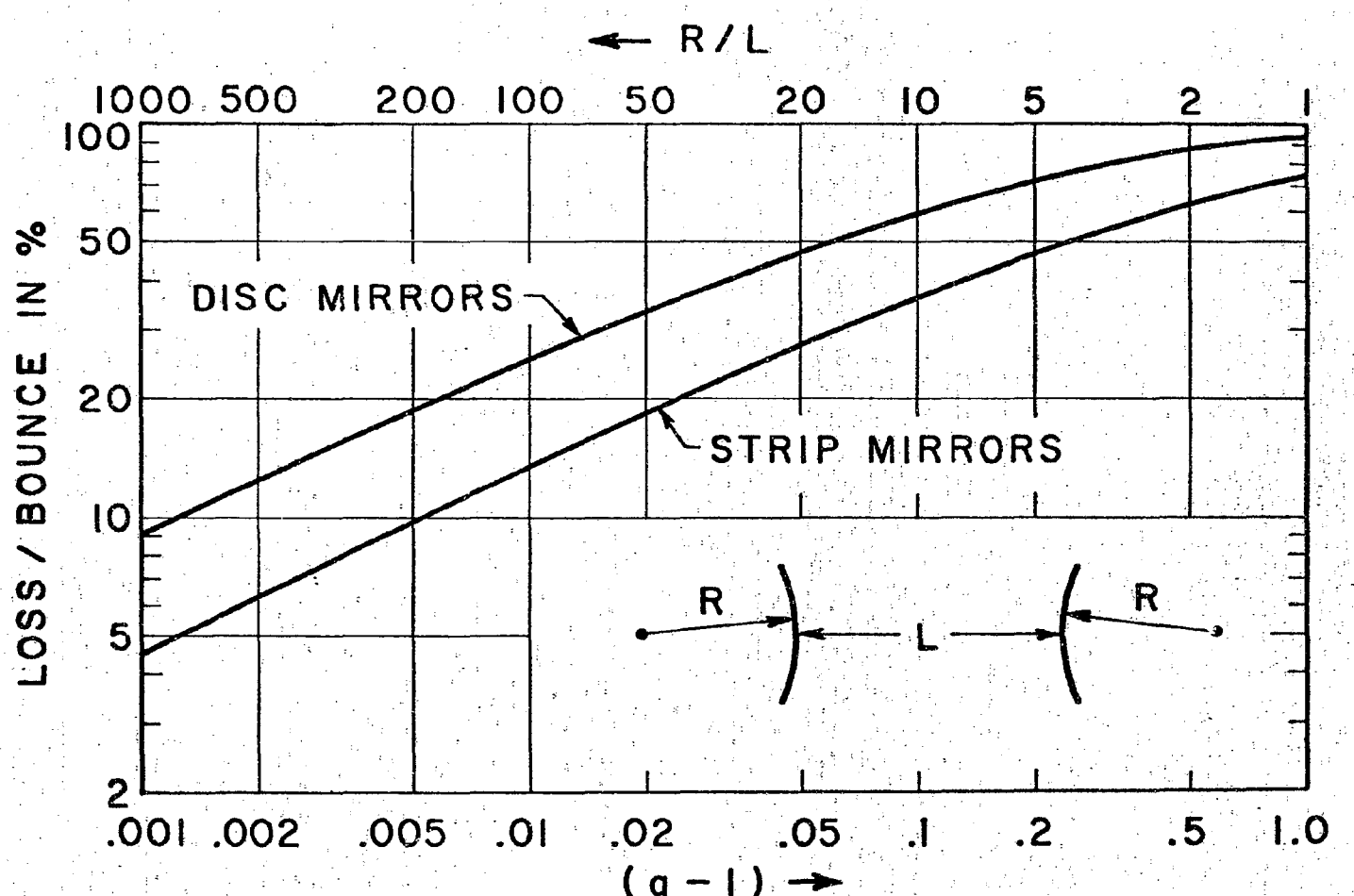

FIG. 4--Average loss per bounce, as defined in the text, vs. mirror curvature for a symmetric unstable optical resonator.

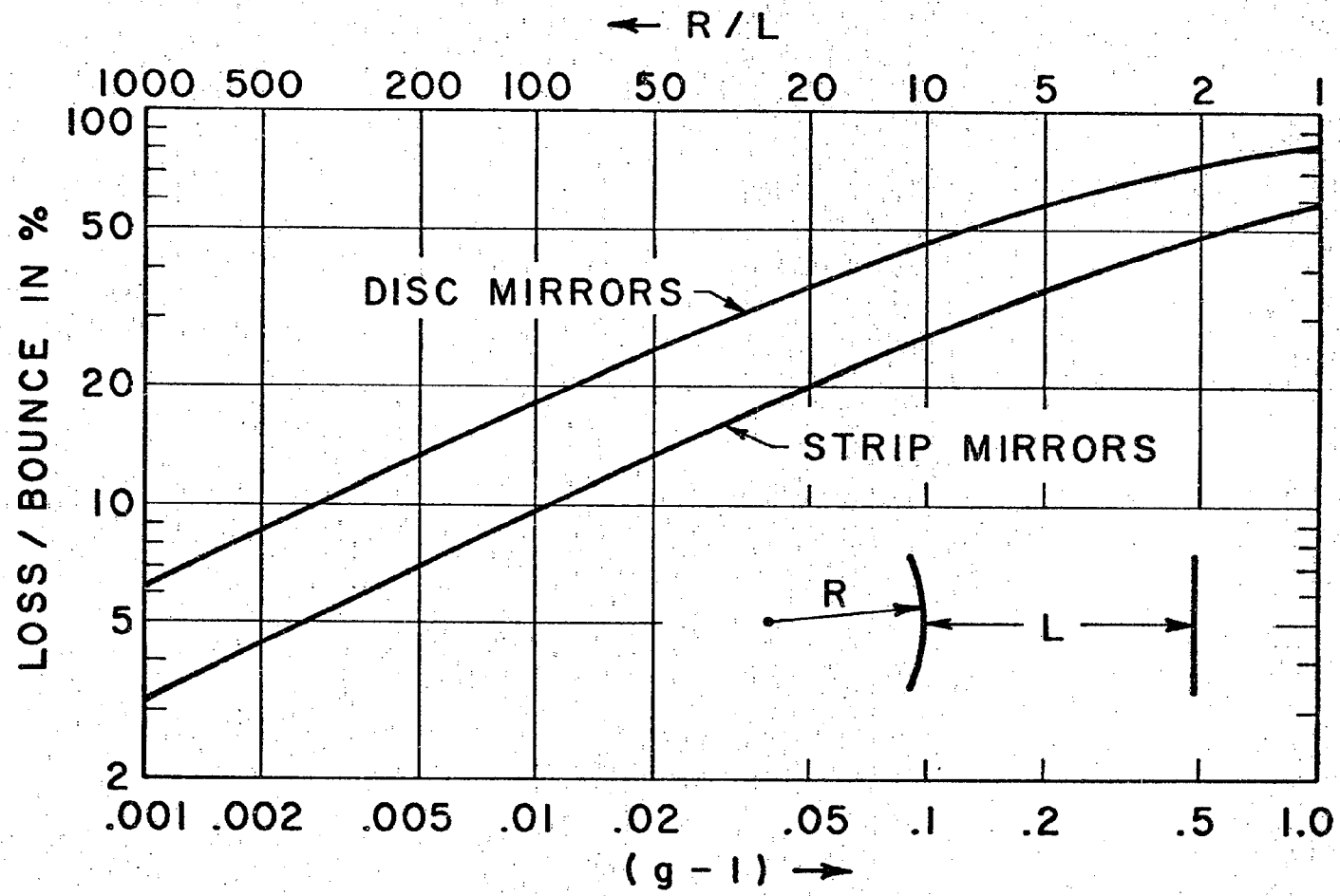

FIG. 5--Average loss per bounce vs. mirror curvature for a half-symmetric unstable optical resonator.

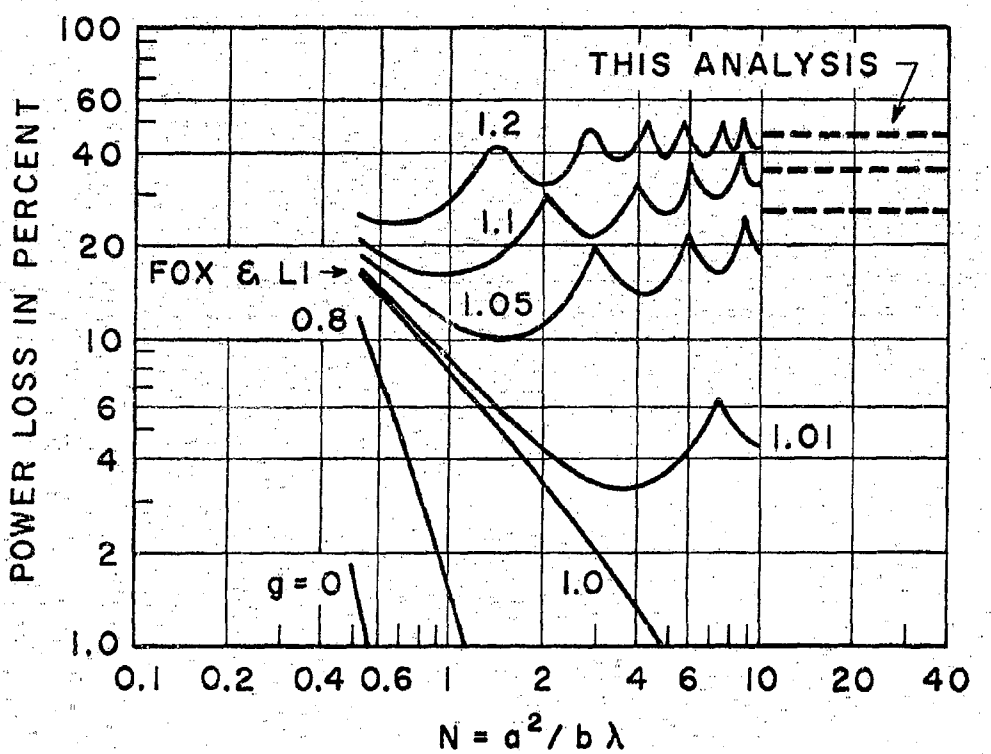

FIG. 6--The solid curves, which are exact results for the infinite strip mirror case for various g values, were obtained by Fox and Li using their iterative numerical approach. The dashed lines are results of the present analysis for the unstable g values 1.05, 1.1, and 1.2.

values approached by the Fox and Li results at large N values. It seems very likely that the periodic ripples as a function of N which can be seen in the Fox and Li results arise from the diffraction effects which are not included in the present analysis.

One can also solve for the contours of constant loss in the g plane by writing

$$\frac{1 - \sqrt{1 - (g_1 g_2)^{-1}}}{1 + \sqrt{1 - (g_1 g_2)^{-1}}} = \pm C \quad ,$$

where $C = \Gamma^2$ for the strip case and Γ for the disc case. Inverting this expression then leads to the result

$$g_1 g_2 = \frac{(1 \pm C)^2}{(1 \pm C)^2 - (1 \mp C)^2} \quad .$$

The constant loss contours are hyperbolae, as shown in Fig. 7, where the contours are labeled by the average loss per pass for the infinite strip mirror case.

We should comment at this point that although sizable diffraction losses are generally necessary in order to obtain transverse mode selection, it is by no means certain that the large losses we have calculated for the unstable region will guarantee transverse mode selection. Indeed, it can be argued that because these losses are primarily geometrical in nature, therefore these diffraction losses will be very nearly the same for the lowest-order and higher-order transverse modes, thus giving little or no transverse mode selection. This question remains to be settled by experiment or by more refined analyses.

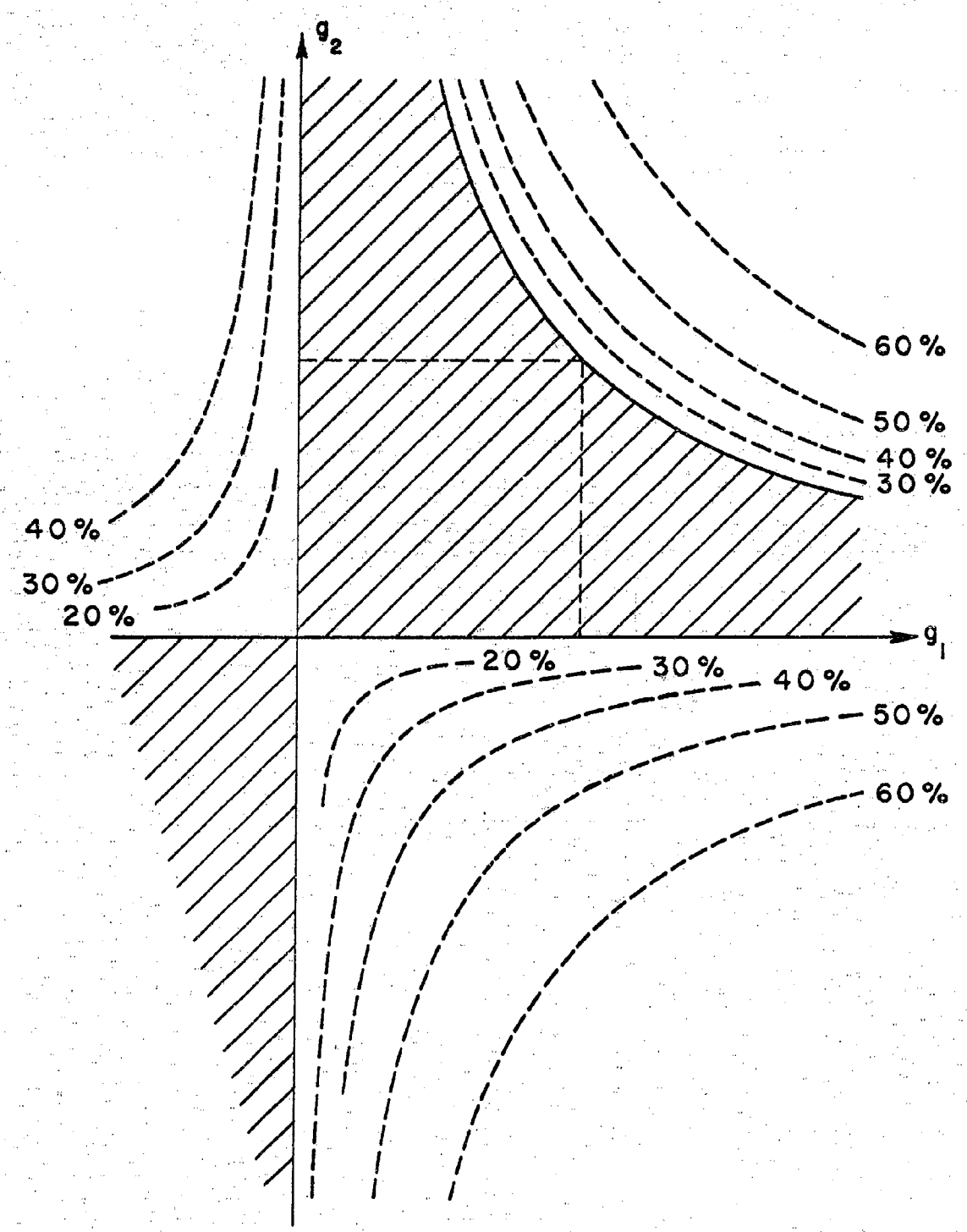

FIG. 7--Equi-loss contours on the mode chart for the infinite strip mirror case. The losses on the same contours for the disc mirror case are substantially larger.

EXPERIMENTAL RESULTS

Experiments on an unstable laser resonator have been carried out using a ruby laser rod which was ground with one flat end surface and one divergent spherical end surface, in the manner of Fig. 5. The results are in good agreement with the present theory. The ruby rod is 5 cm long by 6.35 mm in diameter, with a radius of curvature $R = 1$ meter on the divergent curved end. The curved surface was ground directly on the rod, using brass and then copper convex laps of 15 cm diameter which had been machined to the 1 meter radius of curvature. We elected to grind the divergent surface directly on the laser rod, rather than taking the possibly easier course of using external reflectors, in order to avoid possible difficulties with multiple reflections, and also because the end result is a resonator structure which is as simple and rugged as the ruby rod itself. This rod was prepared before the present theory had been developed. The value of $R/L = 20$ which we selected results in a loss per bounce of $\sim 35\%$, which is perhaps rather more than is desirable. Lower loss rods are now being prepared.

Proper alignment of the laser rod ends was determined using the technique sketched in Fig. 8. A collimated gas laser beam is reflected at normal incidence from the unsilvered front (flat) face and also from the silvered back (curved) face of the ruby rod. Two spots S_1 and S_2 representing the reflections from these two surfaces can then be observed

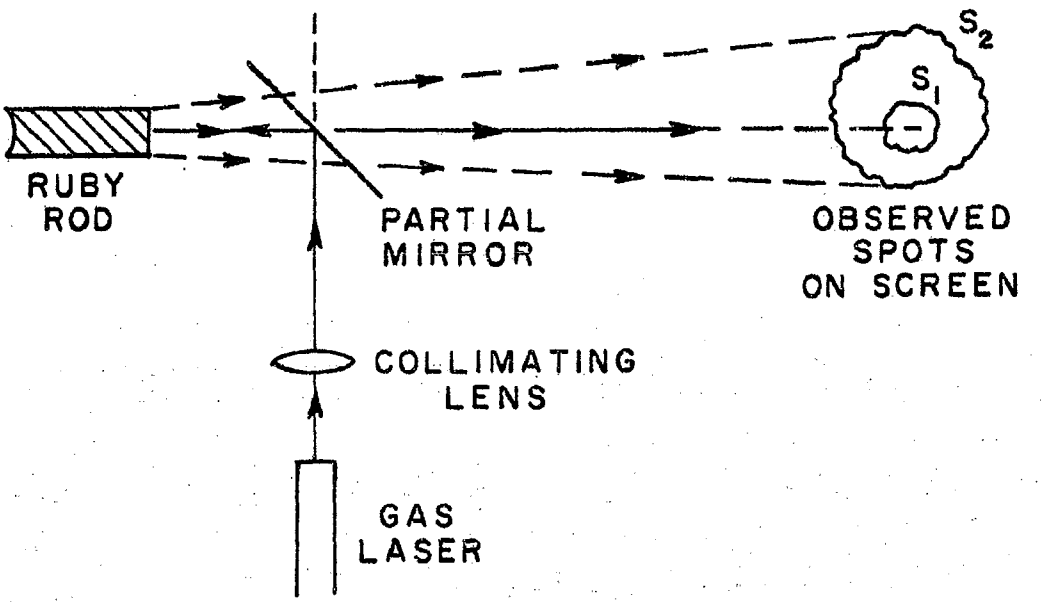

FIG. 8--Experimental technique used to measure the alignment of the end surfaces of the divergent-end laser rod.

on a distant screen, with interference rings similar to Newton's rings present in the overlapping region of the two spots. Coincident centering of the two spots indicates proper alignment of the two faces.

We give in the next few paragraphs some further details of the alignment measurement procedure for those readers who may find this information useful. Figure 9 shows in more detail (and with considerable exaggeration) the geometry necessary in discussing alignment of the rod ends. As shown, a principal optic axis OP is erected in the center of the front face of the laser rod and normal to this face. All coordinates are measured relative to the origin O . As illustrated in the sketch, the barrel of the laser rod may be slightly skew with respect to the optic axis OP . This is essentially irrelevant to the alignment of the rod faces. In the general case, the center of curvature Q of the curved laser end is displaced transversely from the optic axis OP by an amount b , so that the coordinates of point Q are $[-(R + L) , - b]$.

A collimated gas laser wavefront reflected at normal incidence from the front face of the rod will create on a screen placed at distance D from the front face a spot S_1 of the same size as the laser rod and with its center C_1 on the axis OP . The portion of the same incident plane wavefront which is transmitted down the laser rod will reflect from the curved back face of the laser rod as a spherical wave diverging from the point Q' , whose coordinates are $[-(R/2 + L) , - b]$. However, due to refraction at the front face of the laser rod, the spherical wavefront emerging outside the rod will appear to come from the virtual center Q" , whose coordinates are $[- n_0^{-1}(R/2 + L) , - b]$ where $n_0 = 1.76$ is the index of refraction of ruby. This spherical wave, which is apertured

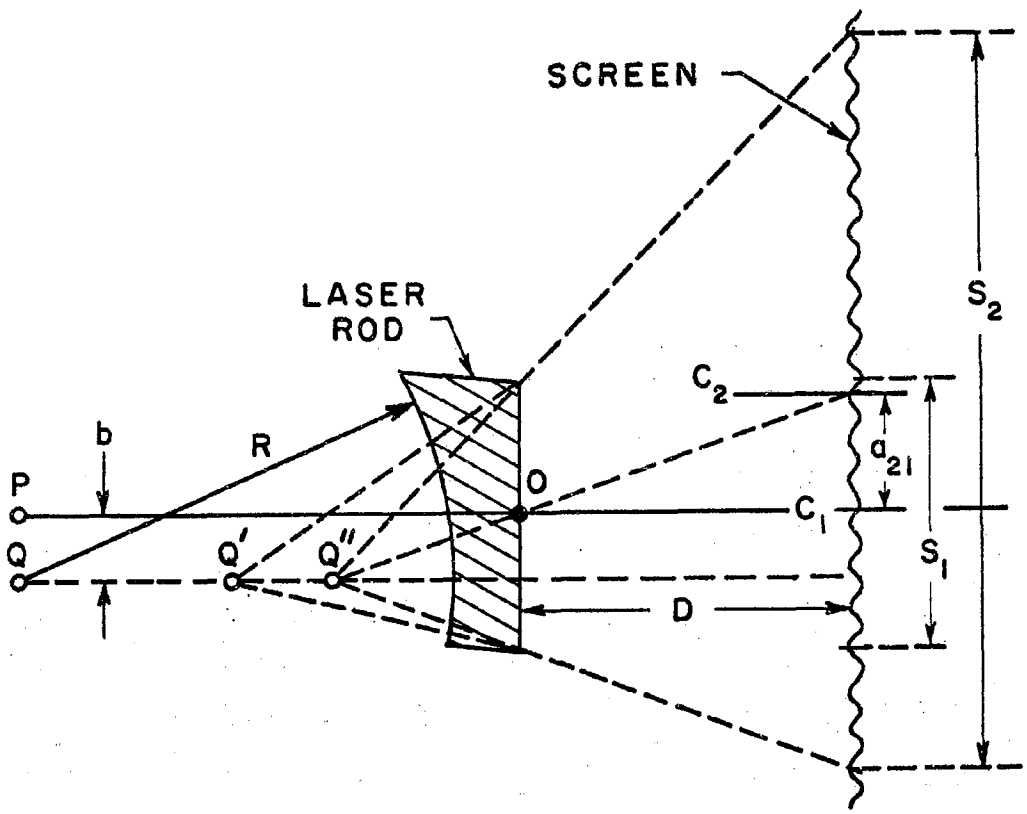

FIG. 9--Geometry used to discuss alignment of the rod ends.

by the front face of the ruby rod, will produce on the screen a larger spot S_2 whose center is point C_2. (We are assuming small angles throughout this discussion. Also, it is not difficult to demonstrate that the conclusions reached here will remain valid even though the monitoring gas laser beam strikes the front rod surface at slightly away from normal incidence.)

From elementary geometry, the diameter $d_2 = 2a_2$ of the large spot S_2 should increase linearly with the screen distance D according to the expression

$$d_2 = 2a_2 = \left[\frac{n_0^{-1} (R/2 + L) + D}{n_0^{-1} (R/2 + L)} \right] 2a \quad ,$$

where $d = 2a$ is the diameter of the laser rod. Experimental verification of this relationship over distances D from 1 to 4 meters served as one verification of the radius of curvature R actually obtained on our laser rod.

In addition, the two centers C_1 and C_2 are displaced from each other by an amount a_{21} given by

$$a_{21} = \frac{D}{n_0^{-1} (R/2 + L)} b$$

Measurement of a_{21} from the spot pattern yields the desired offset

value b, which should approach zero for perfect alignment. The relationship

$$\frac{a_{21}}{a_2} = \frac{D}{D + n_0^{-1}(R/2 + L)} \cdot \frac{b}{a}$$

$$\approx \frac{b}{a}, \quad D \gg n_0^{-1}(R/2 + L)$$

indicates that the offset of the small spot S_1 inside the large spot S_2 on a distant screen is in direct proportion to the offset of the center of curvature Q inside the projected front face of the laser rod.

When first ground, our laser rod had its center of curvature located outside the projected laser front face, giving two completely non-overlapping spots on a distant screen. This was corrected by re-polishing a slight tilt on the flat front face rather than by attempting to correct the curved end. Figure 10 shows two examples of the resulting spot patterns on photographic films located at distances of $D \approx 1$ meter and $D \approx 3$ meters. The larger photograph has been somewhat over-exposed to bring out the weaker large spot reflected from the back surface of the laser rod. This spot exhibits a substantial amount of random structure, presumably due to the optical inhomogeneity of the laser rod which this light has twice traversed. This photograph indicates that the center of curvature of the curved end is offset from the optic axis of the rod by roughly 20% of the rod radius a.

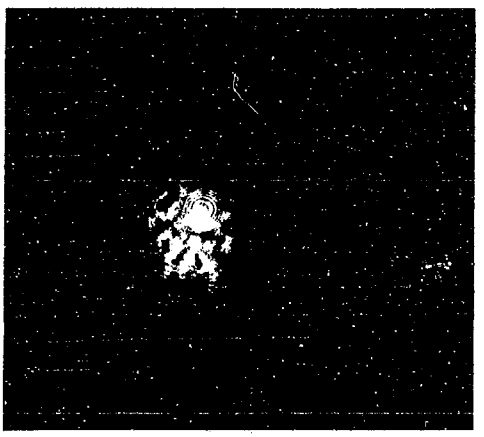

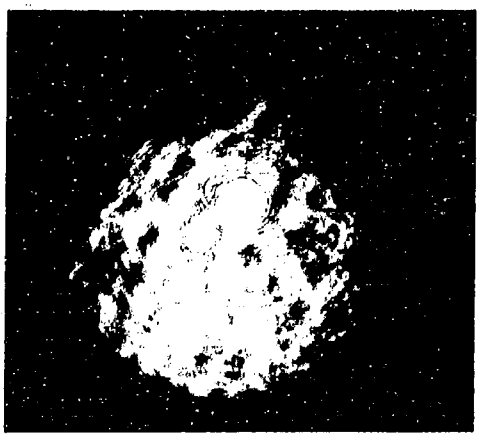

FIG. 10--Two photographs of the spot patterns, obtained by replacing the screen in Fig. 8 with a photographic film. Larger photograph: $D \approx 3$ meters, over-exposed. Smaller photograph: $D \approx 1$ meter, under-exposed.

The smaller photograph in Fig. 10, taken at a smaller distance D, has been somewhat under-exposed to emphasize the interference rings which are observed in the overlap region of the two spots. These rings result from interference between the plane wave reflected from the front face of the rod and the spherical wave reflected from the back face. Figure 9 makes clear that these rings should be centered on the line $QQ'Q''$ and that the center of the rings should be offset inside the smaller spot S_1 by the amount b. The radii of any two successive rings should obey the relationship

$$r_{n+1}^2 - r_n^2 = 2[D + n_0^{-1}(R/2 + L)]\lambda \quad ,$$

where λ is the gas laser wavelength. The visibility or the finesse of these rings might conceivably be used to determine the optical quality of the laser resonator, including optical inhomogeneities in the rod, although this possibility was not explored in our experiments. During alignment a smoothly continuous expansion or contraction of these rings could readily be induced by slightly heating or cooling the laser rod, for example by touching it briefly with a finger.

After alignment, the laser rod was heavily silvered on both ends and tested using a conventional laser pump configuration with an FT-524 flash-tube and surrounding MgO reflector. No laser action could be obtained at room temperature with pump energies up to at least 1200 joules, reflecting perhaps the sizable diffraction losses of this configuration. At $77^{\circ}K$ strong laser action was obtained with a threshold of ~ 500 joules, or approximately the same value as threshold for this rod with more conventional end surfaces.

This particular rod had smoothly polished side walls. At pump levels ~ 20% above the first threshold a number of effects occured indicating the onset of a second type of oscillation. These second oscillations we believe to be some type of light-pipe mode of oscillation involving total internal reflection off the polished side walls, as previously observed by others.[17-19] These effects have also been observed previously with the same rod in other configurations. Measurements for the present discussion were not significantly affected by these oscillations.

The output through the flat, fully silvered end of the laser rod at 77°K was focused to a spot with two different lenses of different focal lengths, in order to determine the virtual center of the output waves by measurement of the axial position of the focused spot. For our configuration, the virtual center P_1' of the output wave, including the effect of refraction at the output face, should be located behind the flat output face by a distance

$$n_o^{-1}\sqrt{(|R|+L)L} = 13.2 \text{ cm}$$

One measurement using a lens of 65 cm focal length gave an experimental value of 14.6 ± 2.0 cm, while a second measurement using a lens of 28 cm focal length gave a value of 13.0 ± 1.3 cm. Both results are thus in good agreement with the theory.

Measurements of the output intensity distribution across the flat end of the fully silvered laser rod were made by taking repeated photographs of the face at the same pump level with successively darker neutral density filters inserted. The laser intensity was generally uniform across the face,

and darkened uniformly in successive photographs. There was a random but reproducible fine structure to the light intensity which may be due to structure in the silver coating or to inhomogeneities in the ruby itself. The laser action was limited to a circular region filling the central 75% to 80% of the laser rod. This fact may be due to the well-known focusing of the pump light into the central 60% of the ruby rod's cross-section, or it may be caused in some way by reflection from the polished sides of the rod. There is every reason to expect some sort of anomalous effects due to side-wall reflection in a polished unstable rod when both ends are fully silvered.

Figure 11 shows what would seem to be a near-optimum configuration for a diffraction-coupled unstable-resonator ruby rod. Both end mirrors in this case are intended to be as nearly totally reflecting mirrors as possible. The mirror on one end is made larger than the spot size on that end. The laser's useful output is then the diffraction-coupled output in the annular ring of laser radiation escaping past the other end. This configuration gives a mode volume which is a large fraction of the available volume of the ruby rod, while at the same time the smaller mirror's size can be adjusted so as to just avoid any contact of the oscillating fields with the side walls of the laser rod, whether these walls are polished or rough. As has been pointed out,[16] although the near-field output in a case like this is an annular ring, the far-field pattern still contains a major lobe directly on axis.

Since the output wave is a divergent spherical wave, collimation of this wave by a lens will be required to obtain a beam of minimum divergence. One can envision the possibility of grinding the necessary curvature for

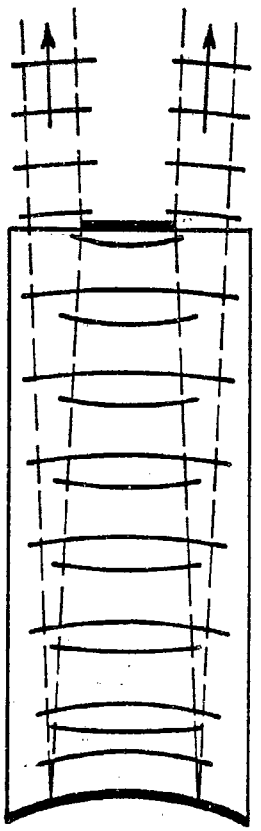

FIG. 11-An unstable resonator configuration for a laser rod which gives a diffraction-coupled output from one end only and which avoids any contact with the resonator side walls.

collimation directly on the ruby rod in the annular region outside the spot, thus eliminating the need for any external lens.

Experiments were conducted on our ruby rod with various smaller mirrors placed on the flat output face in the manner of Fig. 11. Figures 12 and 13 illustrate the resulting output intensities on the flat end of the rod. The upper left-hand photograph in each case is taken below threshold, using the pump light for illumination but with a narrowband filter centered at the ruby wavelength inserted before the camera, so that the photograph is effectively taken using 6900A light. The three succeeding photographs in each case are taken at roughly 10% , 40% and 110% above threshold, with appropriate neutral density filters inserted. No effects due to the second type of oscillation mentioned above were noted in these sequences; whether this second oscillation actually occured is uncertain, since we did not look for any of the other effects it usually causes.

The camera in all cases is focused directly on the front face of the laser rod. The silver spot in Fig. 12 is 2.54 mm in diameter (40% of the rod diameter) and in Fig. 13 is 3.2 mm in diameter (50% of the rod diameter). The surrounding gray spot in the upper left photographs is interpreted to be the more distant and out-of-focus image of the same silver spot as seen reflected in the curved and fully silvered back face of the rod. The spot in Fig. 12 is apparently slightly off-center with respect to the center of curvature of the back face. Several clam-shell chips at the edges of the front face of the rod are apparent in the photographs.

The existence of the predicted halo or diffraction-coupled annular ring of laser light around the silver spot is clearly evident in these photographs. The ratio of the outer diameter of laser action to silver

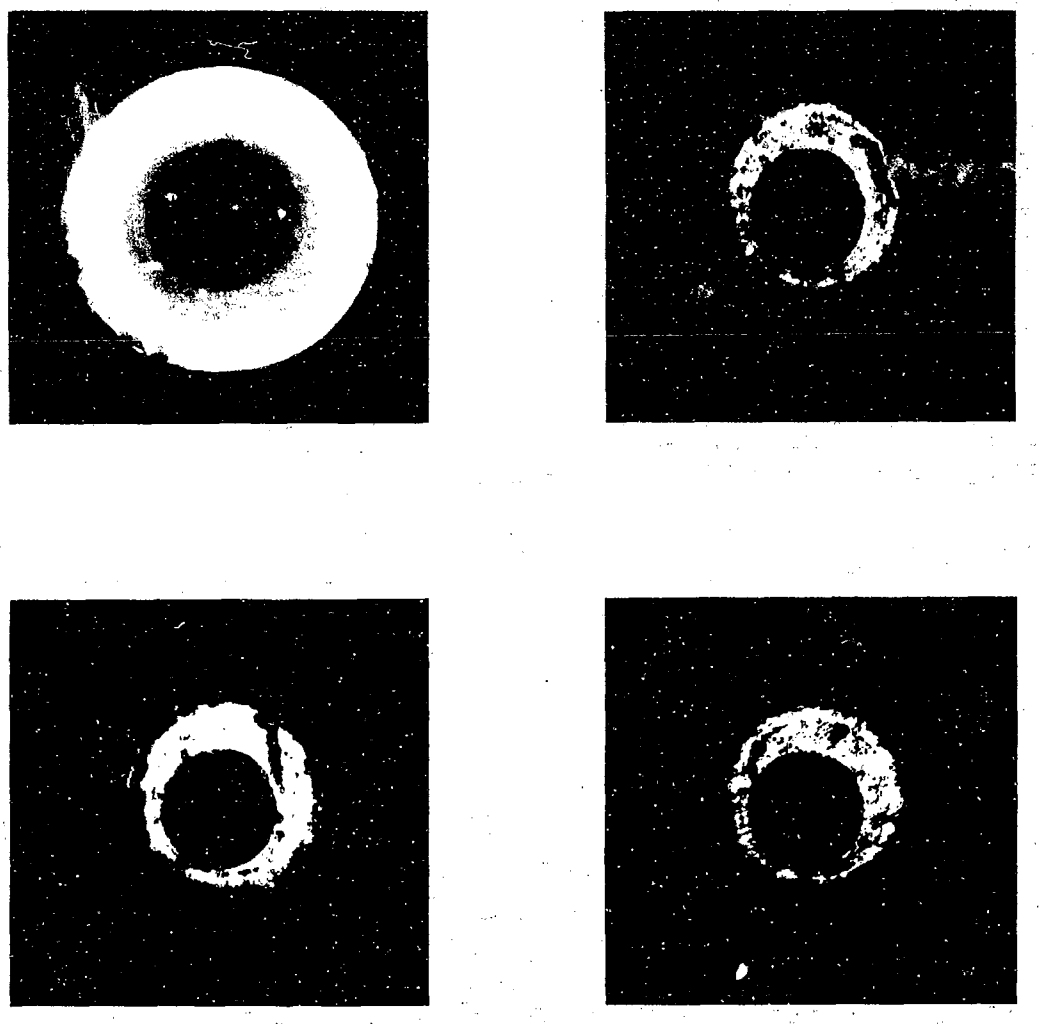

FIG. 12--Photographs of the output end of a ruby rod having the unstable diffraction-coupled resonator configuration shown in Fig. 11. Top left: below threshold, showing the 2-1/2 mm diameter silver spot, plus its mirror image in the opposite end. Succeeding three photographs: laser output at 10%, 40% and 110% above threshold.

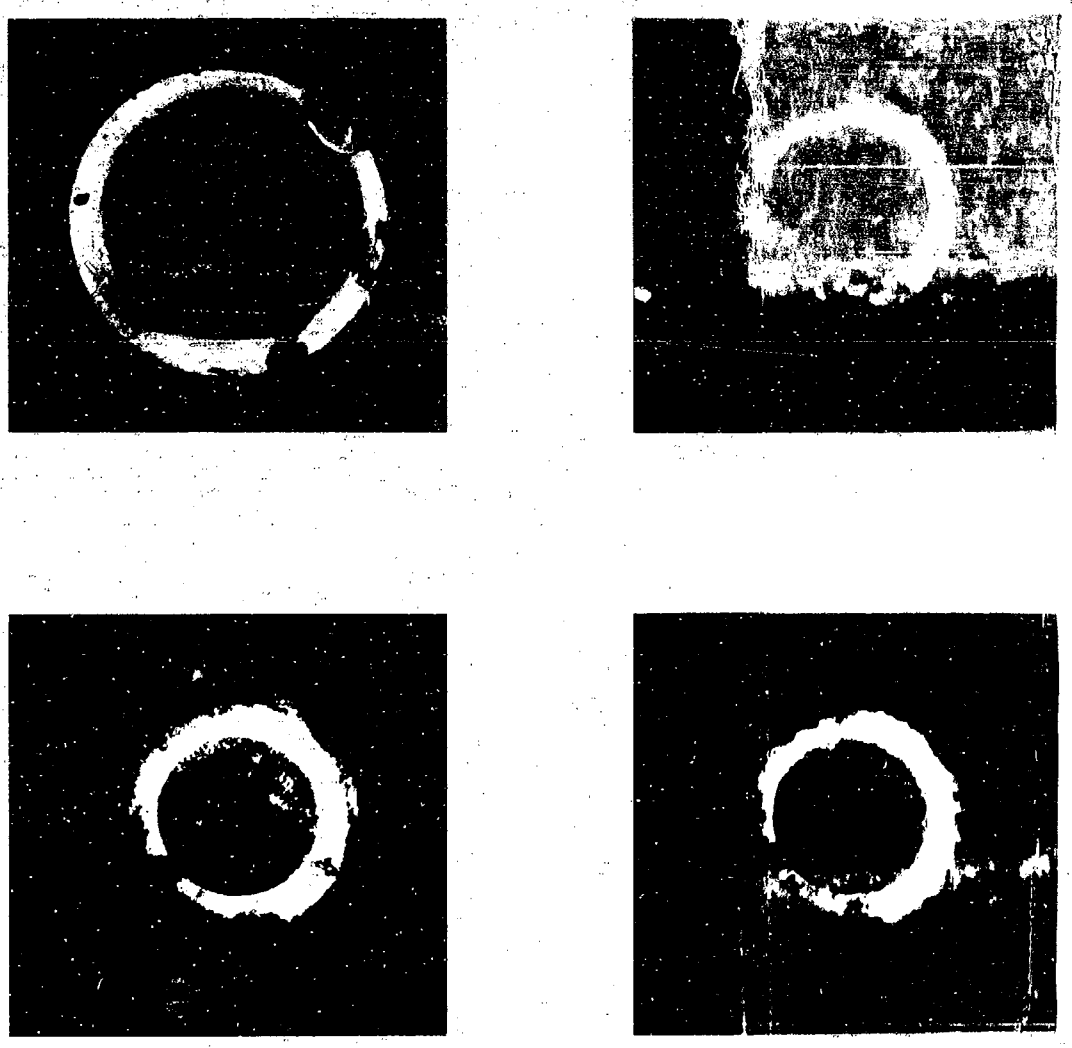

FIG. 13--Same as preceding figure except that the silver [illegible] in diameter (1/2 the rod diameter) and somewhat [illegible] on the rod.

diameter predicted for this rod by the present analysis is 1.55. The experimental values, as well as they can be determined from these photographs, are ~ 1.5 for Fig. 12 and 1.35 to 1.45 for Fig. 13, both of which may be regarded as indicating good agreement with theory. The slight discrepancy in Fig. 13 may be due to nonuniform pumping effects in the ruby rod to a number of other causes or simply to the experimental inaccuracy in these measurements. Note that the gross size and structure of the patterns does not change from near threshold to more than twice threshold. The fine structure in the light output does change to some extent. This may be due in part to varying inhomogeneities in the rod at different pump levels, and to some extent to dust particles on the rod end, as well as to various other causes.

The results which have been presented here are taken to give good confirmation of the unstable resonator theory, at least in its elementary features. Our further experimental efforts on this and similar rods will be chiefly concerned with discovering whether these oscillations occur, as desired, in a single lowest-order diffraction-limited transverse mode.

DISCUSSION AND CONCLUSIONS

As an addendum to the discussions given earlier in this paper concerning transverse mode control and diffraction losses, we wish to advance the following tentative hypotheses. First, the absolute difference in losses and hence the mode discrimination among low-order transverse modes is likely to be small in any resonator with a large Fresnel number, whether the diffraction losses are small as in a stable resonator or large as in an unstable resonator. But, a ruby rod of any reasonable proportions has inevitably a large Fresnel number, making mode selection difficult.

Second, the next higher-order transverse mode in an unstable resonator such as those discussed here, for example in the infinite strip case, is likely to be an asymmetrical mode with very much the same mode pattern and curvatures as the lowest-order mode, but with a null along the resonator axis, a 180° phase shift between the two sides, and a very slightly larger diffraction spreading of the outer edge of the mode.

The third hypothesis is related to this. We propose that if, for example, the mirror on the back or curved end in Fig. 11 is trimmed to just the size of the geometrically predicted spot on that end, then the lowest-order mode will have a slight loss past the edges of this mirror which will be a diffraction loss in the true sense of the phrase. More important, it is proposed that the next higher-order transverse mode will experience a significantly larger diffraction loss past this same edge.

Although these losses will be small compared to the large loss at the opposite end, they may represent sufficient mode discrimination to achieve selection of the lowest-order mode. This type of mode selection, if workable, will have some practical advantages over such methods as the pinhole mode selector, which suffers from breakdown and damage due to the high energy density at the pinhole. Future experimental work will explore this type of mode control.

In general, we conclude that the simple analysis presented here does give a good first-order description of the lowest-order mode and its losses in the general unstable resonator. The analysis has been verified by experiment and by comparison with more exact treatments. Unstable laser resonators may be of practical importance for high-gain lasers, such as ruby laser and other types, particularly in obtaining a diffraction-coupled output.

ACKNOWLEDGEMENTS

It is a pleasure to acknowledge the helpful contributions to the experimental measurements which were made by James G. O'Brien and James W. Allen, and to the fabrication of the curved end rod which was done by Forrest Futtere. The suggestion of trying a divergent end rod for transverse mode control was first made to the author more than a year ago by Prof. Arthur Schawlow. We appreciate the support of this work by Contract DA 36(039) SC-90839 from the U. S. Army Electronics Command, Fort Monmouth, N. J.; and by Contract AF 33(615)-1411 from the U. S. Air Force Avionics Laboratory, Wright-Patterson AFB, Ohio.

REFERENCES

1. A. G. Fox and T. Li, Proc. IRE 48, 1904 (1960).
2. A. G. Fox and T. Li, Bell Sys. Tech. J. 40, 453 (1961).
3. A. G. Fox and T. Li, Proc. IEEE 51, 80 (1963).
4. A. G. Fox and T. Li, "Modes in a maser interferometer with curved mirrors," Quantum Electronics III. (Columbia University Press, New York, 1964), vol. 2, p. 1263.
5. G. D. Boyd and J. P. Gordon, Bell Sys. Tech. J. 40, 489 (1961).
6. G. D. Boyd and H. Kogelnik, Bell Sys. Tech. J. 41, 1347 (1962).
7. S. R. Barone, J. Appl. Phys. 34, 831 (1963, Part I).
8. S. P. Morgan, IEEE Trans. MTT-11, 191 (1963).
9. R. F. Soohoo, Proc. IEEE 51, 70 (1963).
10. P. Szulkin, Bull. Acad. Poln. Sci. Ser. Sci. Tech. (Poland) 8, 630 (1960).
11. C. L. Tang, Appl. Optics 1, 768 (1962).
12. A. G. Fox, et al, Appl. Optics 2, 544 (1963).
13. L. A. Vainshtein, Sov. Phys. - JETP, 17, 709 (1963).
14. L. A. Vainshtein, Sov. Phys. - JETP 18, 471 (1964).
15. L. Bergstein and H. Schachter, J. Opt. Soc. Am. 54, 887 (1964).
16. J. T. LaTourette, S. F. Jacobs, and P. Rabinowitz, Appl. Optics 3, 981 (1964).
17. A. Szabo and F. R. Lipsett, Proc. IRE 50, 1690 (1962).

18. W. R. Sooy, R. S. Congleton, B. E. Dobratz, and W. K. Ng, "Dynamic limitations on the attainable inversion in ruby lasers," Quantum Electronics III (Columbia University Press, 1964), vol. 2, p. 1103.

19. R. J. Collins, and J. A. Giordmaine, "New modes of optical oscillation in closed resonators," Quantum Electronics III. (Columbia University Press, 1964), vol. 2, p. 1239.

20. T. Li, Private communication.

SCIENTIFIC AND TECHNICAL INFORMATION FACILITY

operated for National Aeronautics and Space Administration by Documentation Incorporated

LOAN DOCUMENT TRANSMITTAL

Please attach a copy of this form to any loan documents sent to the Scientific and Technical Information Facility. A single copy of this form and the document should be sent to the following address:

Scientific and Technical Information Facility
Attention: NASA Representative
Box 5700
Bethesda 14, Maryland

Every effort will be made to return this document in the shortest possible time.

Please complete. Date sent: NOV 17 1964

Sent by: NATIONAL AERONAUTICS AND SPACE ADMINISTRATION
LEWIS RESEARCH CENTER
21000 BROOKPARK RD.
CLEVELAND 35, OHIO
ATT: LIBRARY

☑ checked for N numbers ☑ checked against N-62 numbers

See other side for NASA contractor report

For Facility Use Only

LOAN DOCUMENT PROCESSING RECORD

N62-_____ Date received: 11-24

X62-_____

THIS DOCUMENT IS ON LOAN

Please process as follows:	Date	Initials
☐ Film for Microform and make Xerox copy		
☐ Microform completed		
☐ Xerox copy made		
☐ Xerox copy sent to Input Station		
☐ Original sent to Mail Room		
☐ Document returned to sender		

12996

THIS LOAN DOCUMENT FORM MUST BE SENT TO THE CASE FILE

Facility Test Form 443, Sept. 1962

COMPLETE FOR NASA CONTRACTOR DOCUMENTS ONLY

DOCUMENT TYPES

1. _____ Report is unclassified and is suitable for unlimited announcement and distribution to the aeronautics and space community, and for public sale.

2. _____ Report is unclassified, but contains information of limited usefulness and does not justify widespread automatic distribution to the aeronautical and space community. It can, however, be announced and made publicly available.

3. _____ Report is unclassified, but for official reasons, must be restricted as follows:

   a. _____ Government agencies and their contractors only.
   b. _____ Government agencies only.
   c. _____ NASA activities only.

4. _____ Report bears a security classification and is suitable for distributio within the limits of security considerations to:

   a. _____ Government agencies and their contractors only.
   b. _____ Government agencies only.
   c. _____ NASA activities only.

5. _____ Reprint of a journal article reporting NASA-supported work.

6. _____ Article prepared for journal publication (preprint or other copy) reporting NASA-supported work. (Normally handled as No. 2 above.)

   Estimated date of publication: _____

7. _____ Material for presentation at a meeting or conference
   Name of Meeting: _____ Date: _____
   Sponsor(s): _____

   a. _____ Scheduled for publication in proceedings. (Normally handled as No. 2 above.)

      Estimated date of publication: _____

   Not scheduled for publication in proceedings and subject to the following limitations or announcement and dissemination:

   b. _____ Government agencies and their contractors only.
   c. _____ Government agencies only.
   d. _____ NASA activities only.